MICE: AN IMPLICIT DIFFERENCE SCHEME FOR MHD CALCULATIONS

Frederic E. Fajen

Mission Research Corporation

Prepared for:

Defense Nuclear Agency

March 1973

DNA 2877Z
MARCH 1973
MRC-R-12

MICE
AN IMPLICIT DIFFERENCE SCHEME FOR MHD CALCULATIONS

Fredric E. Fajen

Headquarters
Defense Nuclear Agency
Washington, D.C. 20305

Mission Research Corporation
One Presidio Avenue
Santa Barbara, California 93101

Contract No. DASA01-71-C-0054

ACKNOWLEDGEMENT

I wish to thank Reagan W. Moore and D. Christine Moore for their very valuable help in the coding and over-all organization of the MICE code.

SECTION I

INTRODUCTION

MICE is an implicit, time-step-split, MHD code which is being developed at Mission Research Corporation to extend and improve upon our capability to compute the late-time phenomenology of high altitude nuclear explosions. The code has been designed to do calculations in one-dimensional spherical, 1-D planar, 2-D cartesian, 2-D cylindrical, or 3-D cartesian geometry.

In addition to computing an approximate numerical solution to the one-fluid MHD equations, the code also calculates the following for each space point and for each time, (1) the Lagrangian coordinate, (2) the number densities of the atmospheric species N_2, O_2, N, O, N^+, O^+, and an "all-purpose" molecular ion X_2^+, and (3) the rate of energy loss by radiation of UV. There is a deposition routine which may be called one or more times during the running of a problem, to deposit x-rays and/or UV radiation. A very general rezoning routine allows a problem to be transferred to any new grid at any time during the running of the problem. These "phenomenology" aspects of the code have been patterned after the MRC code HOIL, which has been described in reference 1.

The DNA sponsored high-altitude phenomenology community already has several codes which calculate late-time phenomenology. There are two-dimensional codes at LASL, NRL, and MRC, and three-dimensional codes at AFWL and NRL. These codes all use explicit difference techniques. The characteristic feature of such difference techniques is that

numerical stability considerations impose the condition that the mesh speed, $\Delta x/\Delta t$, must exceed the physical signal propagation speed, $U + C$, where U is the magnitude of the fluid velocity, and C is the speed with which waves travel through the fluid. The corresponding requirement for implicit codes, such as MICE, is simply $\Delta x/\Delta t > U$. For strong shock problems, where U and C are comparable in magnitude, the two type of codes require comparable running times. However, for problems involving subsonic flow, such as low altitude fireball rise, or the late-time stages of high altitude atmospheric heave, the implicit type of code will be able to use much larger time steps, and therefore, require much less computer time. It is the need for shorter running times for high altitude heave calculations which has prompted the development of MICE. In the ROSC code (Radar and Optical Systems Code) it will, of course, be necessary to have a reliable model of atmospheric heave. One possibility for this "model", is to use a coarsely zoned 3D MHD code as an integral part of ROSC. If this is to be done, the MHD scheme which is used will need to be as efficient and fast running as possible. An implicit code, such as MICE, is needed to meet these requirements.

Another distinctive feature of MICE is its use of the approximation of time-step-splitting. This greatly simplifies the coding, makes it easier to implement changes in the difference scheme, reduces the main core requirements, and gives the code the ability to do calculations in several different geometries. This aspect of the code is discussed further in section 3 of this report, which deals with the details of the difference scheme.

Unclassified
Security Classification

DOCUMENT CONTROL DATA - R & D

(Security classification of title, body of abstract and indexing annotation must be entered when the overall report is classified)

1. ORIGINATING ACTIVITY (Corporate author)	2a. REPORT SECURITY CLASSIFICATION
Mission Research Corporation One Presidio Avenue, P.O. Drawer 719 Santa Barbara, California 93101	Unclassified 2b. GROUP

3. REPORT TITLE

MICE, AN IMPLICIT DIFFERENCE SCHEME FOR MHD CALCULATIONS

4. DESCRIPTIVE NOTES (Type of report and inclusive dates)

Interim Report

5. AUTHOR(S) (First name, middle initial, last name)

Frederic E. Fajen

6. REPORT DATE	7a. TOTAL NO. OF PAGES	7b. NO. OF REFS
March 1973	48 38	5

8a. CONTRACT OR GRANT NO.	9a. ORIGINATOR'S REPORT NUMBER(S)
DASA01-71-C-0054	MRC-R-12
b. PROJECT NO NWER: H	
c. Task and Subtask: C062	9b. OTHER REPORT NO(S) (Any other numbers that may be assigned this report)
d. Work Unit: 11	DNA 2877Z

10. DISTRIBUTION STATEMENT

Approved for public release; distribution unlimited

11. SUPPLEMENTARY NOTES	12. SPONSORING MILITARY ACTIVITY
	Director Defense Nuclear Agency Washington, D.C. 20305

13. ABSTRACT

This report describes the MICE code, which uses a new numerical technique for solving the one fluid MHD equations. Although the technique evolved from some of the general ideas developed by Harlow and Amsden in their ICE (Implicit, Continuous-Fluid, Eulerian) method, it has been extensively modified, and is best described as an implicit Lax-Wendroff technique. The approximation of time-step-splitting is used, which greatly simplifies the numerical solution.

Some numerical results are presented for two test problems. The MICE computation of the early expansion and rise of a hot bubble in an exponential atmosphere is compared to previously published calculations of the same problem. The buoyant rise of a warm infinitely long cylinder is calculated and the shape of the boundary is compared to an exact solution obtained by G. McCartor of MRC. The agreement is satisfactory in both cases.

DD FORM 1 NOV 68 1473

I

Unclassified
Security Classification

14 KEY WORDS	LINK A		LINK B		LINK C	
	ROLE	WT	ROLE	WT	ROLE	WT
NUCLEAR WEAPONS						
HIGH ALTITUDE PHENOMENOLOGY						
MHD CALCULATIONS						
IMPLICIT DIFFERENCE SCHEME						

SECTION II

SOME NUMERICAL RESULTS

Here we present the results of two test calculations. The first calculation is that of the early expansion and rise of a hot bubble in an exponential atmosphere. Some comparisons are made with other numerical solutions of the same problem. The second calculation is that of the buoyant rise of a warm cylinder.

HOT BUBBLE PROBLEM

This problem was chosen as a test case, because numerical solutions of the same problem have been published by Harlow and Meixner[2] and by Sappenfield[3]. The initial conditions are as follows: 8.2×10^{20} ergs of energy are placed within a sphere of 2.7 km radius. The velocity within the sphere is taken to be directed radially outward from the center, and to have the magnitude $v = 4.25 \left[1 + \frac{\Delta h}{6\text{km}}\right]$ km/sec, in which Δh is the vertical displacement from the burst point. The internal energy within the sphere is 8×10^{12} ergs/gm. Burst point mass density is 1.2×10^{-9} gm/cc, and the atmospheric scale height is 6 km. In the MICE calculation, the grid spacing was initially chosen as $\Delta R = \Delta Z = .4$ km. At $t = .45$ sec, the problem was rezoned into a grid with $\Delta R = \Delta Z = 1$ km.

A numerical solution to this problem was obtained by Harlow and Meixner with a particle-in-cell (PIC) code, and later by Sappenfield with a mixed Eulerian-Lagrangian code called H2SE. Figure 1 shows the shock position as a function of time for the three directions, "down", "sideways", and "up", as calculated by PIC, H2SE, and MICE. Of the three calculations, the H2SE result is probably the most reliable,

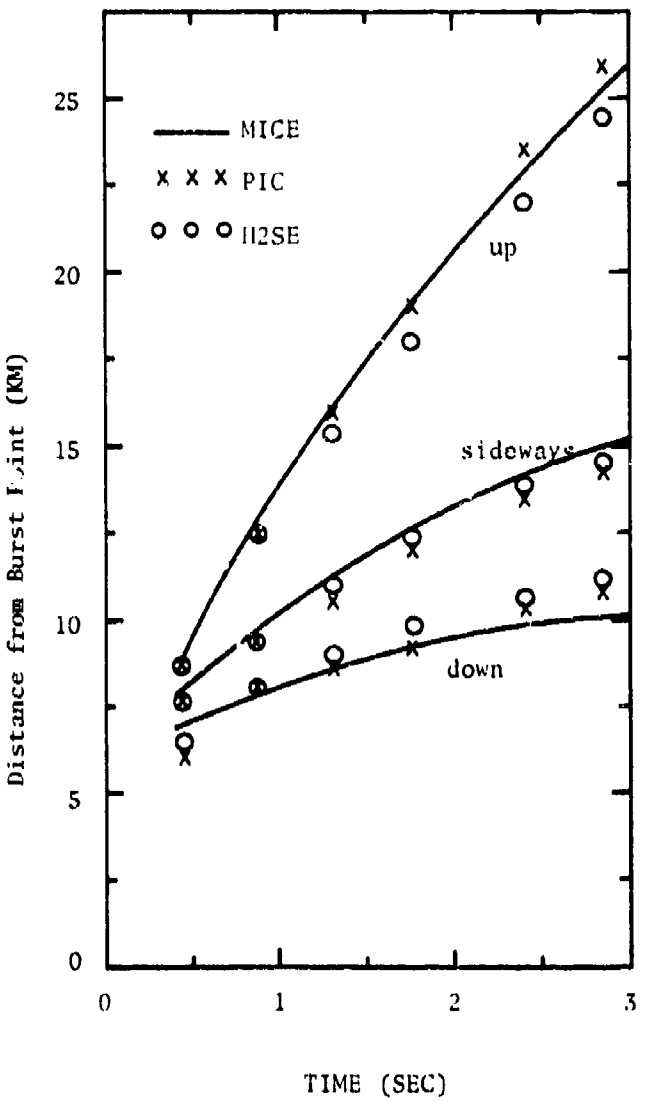

Figure 1. Shock positions as a function of time for the hot bubble problem.

since H2SE has Lagrangian boundaries perpendicular to the direction of shock propagation. Lagrangian codes usually give better definition of shock positions than do Eulerian codes.

Figure 2 shows contour of mass density as given by H2SE and MICE. The two sets of contours agree qualitatively very well. The lack of detailed agreement is caused by the fact that MICE is an Eulerian code, and used a mesh spacing of 1 km for this problem.

BUOYANT RISE OF A WARM CYLINDER

Recently, at MRC, an analytic solution has been obtained for the early buoyant rise of a cylinder of imcompressible fluid of mass density ρ_1 , imbedded in another fluid of density $\rho_0 > \rho_1$, in a gravitational field[4]. This solution was obtained by expanding the fluid equations for inviscid, imcompressible flow, in a power series in time, and is an exact solution for as long as the power series converges. We give here a comparison of the analytic solution for the case $\rho_1 = .5\,\rho_0$, and a similar problem which was run with the MICE code.

The initial conditions for the MICE problem were chosen as follows:

ambient mass density $\rho_0 = 8.9\times10^{-5}$ gm/cc
density scale height $H_s = 6.3\times10^{5}$ cm
ambient specific internal energy $I_0 = 1.53\times10^{9}$ erg/gm
specific heat ratio $\gamma = 1.4$
initial cylinder radius $R = 5\times10^{4}$ cm

Inside the cylinder the mass density was taken to be .5 x ambient density, and the internal energy 2.0 x ambient internal energy. The problem was run in 2-D Cartesian geometry, with a minimum cell size of about .1 R.

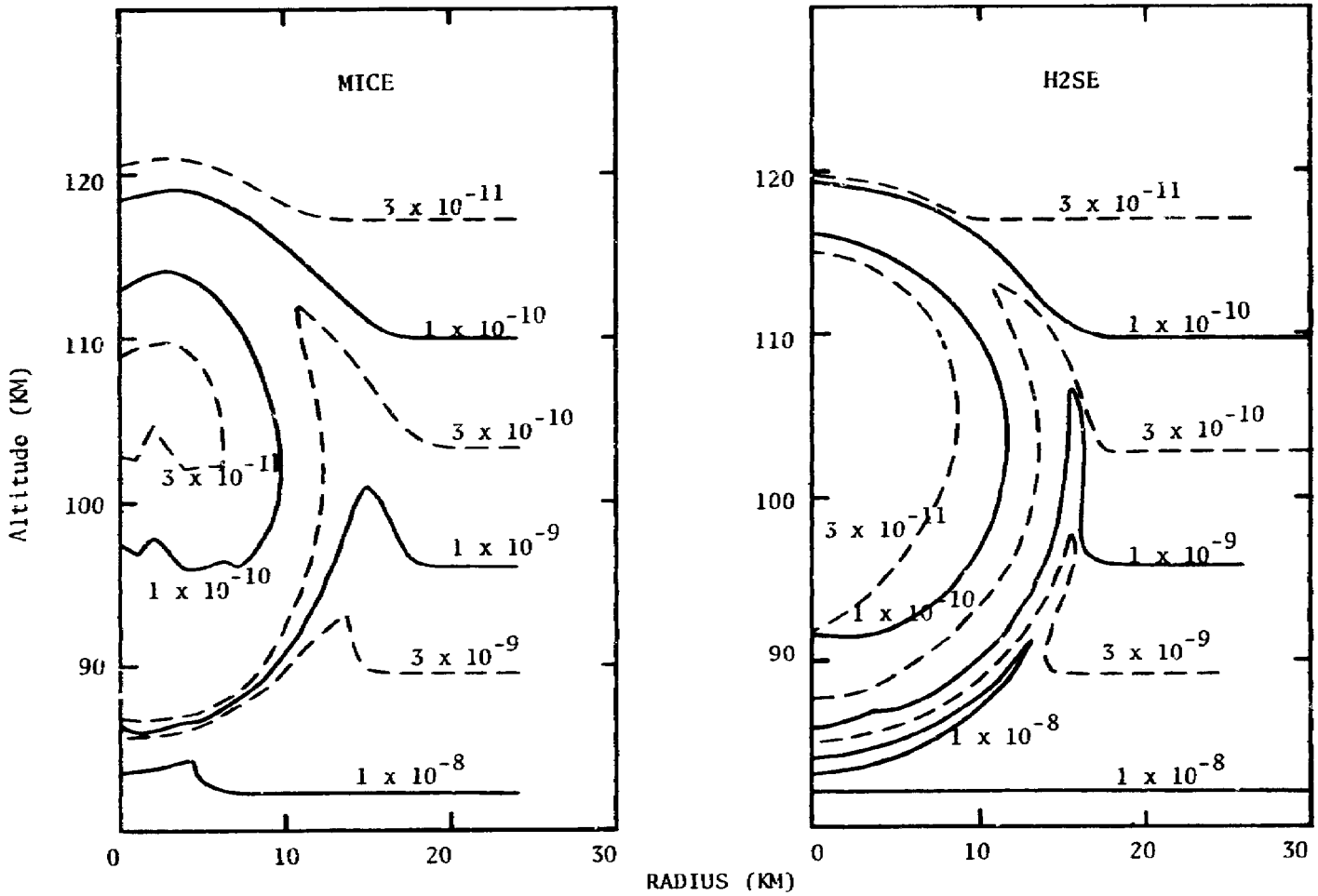

Figure 2. Contours of mass density at t = 2.85 sec for the hot bubble problem.

This problem, as done by the MICE code, is, of course, a compressible flow problem, since the sound speed is finite. Also, since this code, like all fluid codes, has inherent numerical viscous effects, the problem being reported here is clearly a different problem than that for which we have the analytic solution. However, if the sound speed is sufficiently large, and if the numerical viscous effects do not dominate the problem, we would expect the results to be not too different from the analytic results. To see how large the sound speed is in the context of this problem, it is useful to work in an appropriate set of dimensionless units.

The power series expansion for the height of the center of mass of the cylinder as a function of time is

$$h = \frac{\rho_0 - \rho_1}{\rho_0 + \rho_1} \frac{1}{2} g t^2 + \text{higher order terms},$$

which may be written in dimensionless form as

$$H = \frac{h}{R} = \frac{1}{2}\left(\frac{t}{\sqrt{R/g'}}\right)^2 + \ldots = \frac{1}{2} T^2 + \ldots ,$$

where $g' = \frac{\rho_0 - \rho_1}{\rho_0 + \rho_1} g$.

R is the initial radius of the cylinder, and g is the acceleration of gravity. If c is the sound speed in cgs units, then the dimensionless sound speed is:

$$C = c \times \frac{1}{R} \times \sqrt{R/g'} = c/\sqrt{R\, g'} \quad .$$

For the set of initial conditions given above, the sound speed inside the cylinder is

$$C = \left[\gamma(\gamma-1)x2I_0/(R\, g')\right]^{\frac{1}{2}} = 10.3$$

Thus, a sound signal can traverse the radius of the cylinder about 10 times in the time required for the cylinder to rise a distance of $\frac{1}{2}$ R . We would therefore expect "compressibility" effects to be relatively minor. The numerical viscosity effects are more difficult to assess, and we have made no attempts to do so.

Figure 3 shows a comparison of the position of the boundary of the cylinder at $T^2 = 1.5$. The analytic solution fails to converge for times much beyond this time. The MICE boundary agrees reasonably well with the analytic solution, although it tends to oscillate about the analytic result. Figure 4 shows the best MICE calculation we could get for this problem. Here, we used a minimum cell spacing of about .05 R, with a corresponding decrease in Δt.

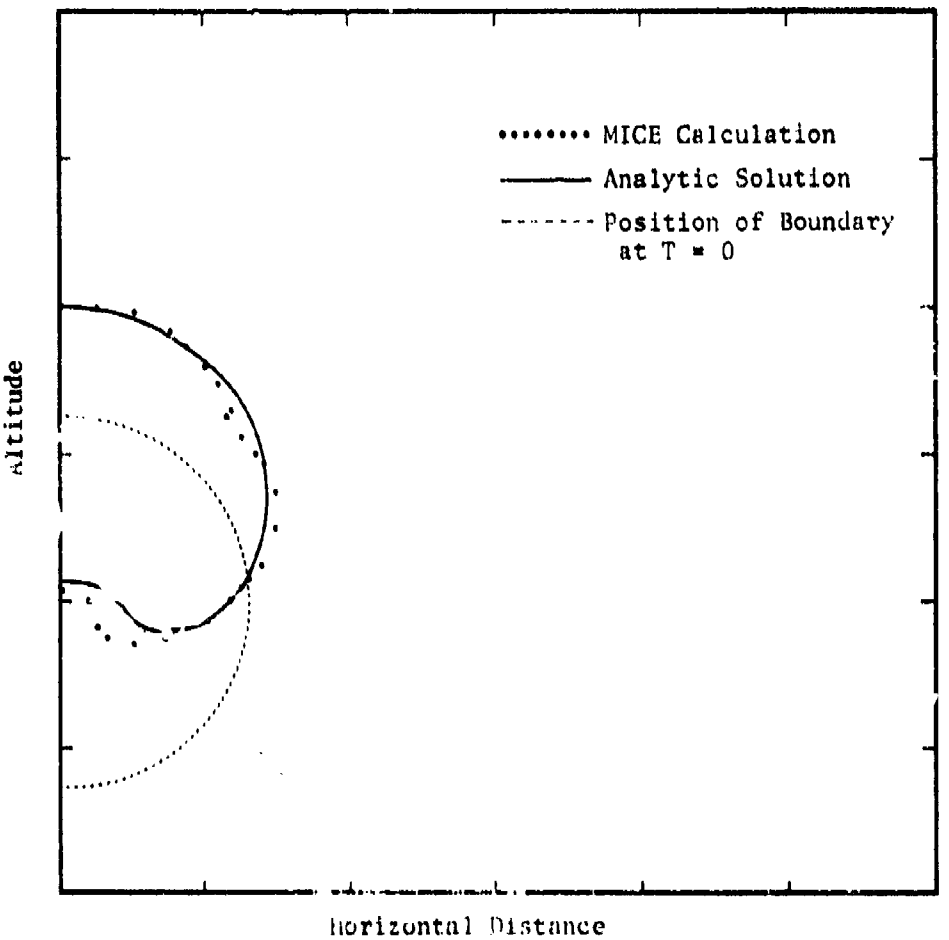

Figure 3. MICE Calculation of the Buoyant Rise of a Warm Cylinder, with Minimum $\Delta X \simeq R/10$.

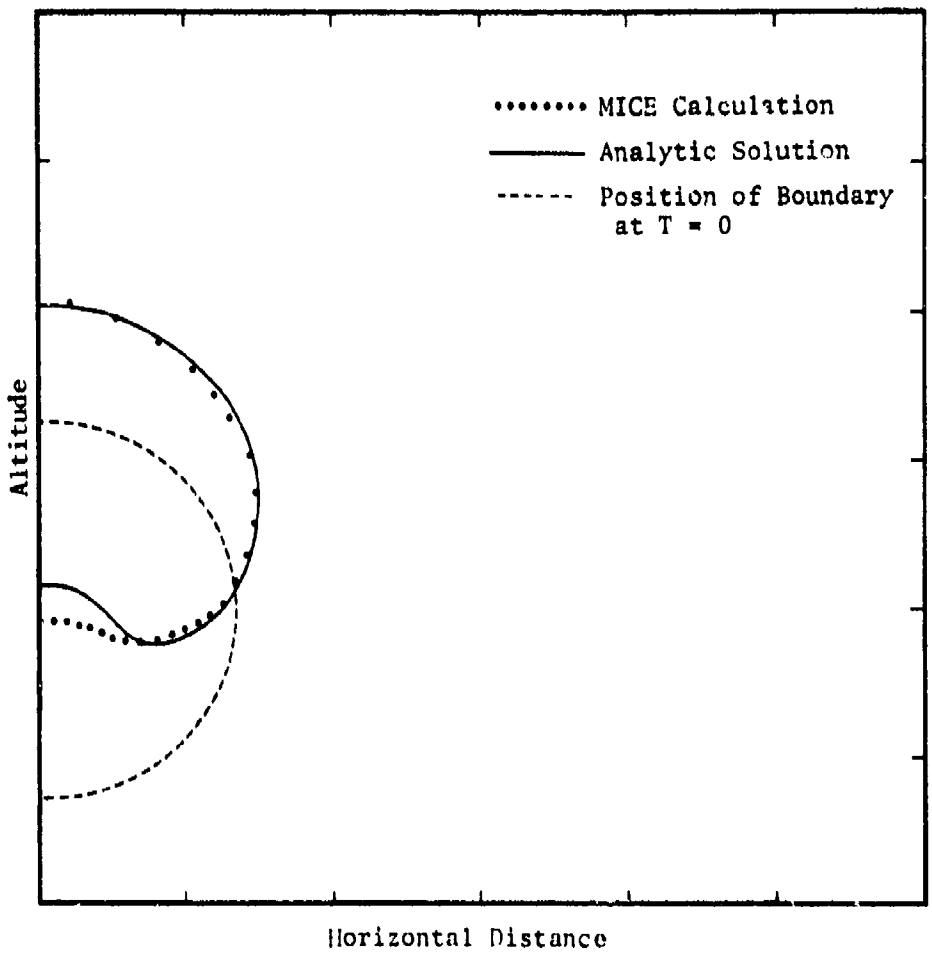

Figure 4. MICE Calculation of the Buoyant Rise of a Warm Cylinder, with Minimum $\Delta X \simeq R/20$.

SECTION III

THE NUMERICAL DIFFERENCE SCHEME

In this section of the report, the MICE numerical difference scheme is described. The starting point of this description is a presentation of the set of partial differential equations used in MICE for the flow of an infinitely conducting fluid. The approximations used in the difference equations are then given. The concept of difference operators is used to explain what is meant by time-step-splitting and the MICE difference operator is then described in sufficient detail so that the interested reader can understand the numerical scheme.

Two topics not discussed in this report are the MICE transport of chemical species and Lagrangian coordinates. Information on the Lagrangian coordinates is contained in Reference 1 which discusses the idea of Lagrangian coordinates in an Eulerian code and gives a first order scheme for advancing the quantities in time.

DIFFERENTIAL EQUATIONS

$$\frac{\partial \rho}{\partial t} = - \nabla \cdot \left(\rho \vec{v}\right) \tag{1}$$

$$\frac{\partial (\rho \vec{v})}{\partial t} = - \nabla \cdot \left(\rho \vec{v}\vec{v}\right) - \nabla \left(p + \frac{B^2}{2}\right) + \left(\vec{B} \cdot \vec{\nabla}\right) \vec{B} - \rho g \hat{e}_z \tag{2}$$

$$\frac{\partial \vec{B}}{\partial t} = \vec{\nabla} \times \left(\vec{V} \times \vec{B} \right) \tag{3}$$

$$\frac{\partial}{\partial t} (\rho I) = - \vec{\nabla} \cdot \left(\rho I \vec{V} \right) - P \left(\vec{\nabla} \cdot \vec{V} \right) \tag{4}$$

$$P = (\gamma - 1) \rho I \tag{5}$$

where ρ is the mass density in gm/cc, $\vec{V}$ is the fluid velocity in cm/sec, P is the fluid pressure in dynes/cm^2, $\vec{B}$ is the magnetic field strength in $\sqrt{4\pi}$ gauss, I is the specific internal energy in ergs/gm, and γ is the specific heat ratio.

APPROXIMATIONS

The collection of all values of ρ, $\rho\vec{V}$, $\vec{B}$, ρI, $\vec{R}_L$, $\{n_i\}$ at all points in the space mesh can be considered to be the components of a multi-dimensional vector $\underline{U}$. An explicit difference approximation to the differential equations has the form

$$\underline{U}^{n+1} = \underline{U}^n + L_x(\underline{U}^n) + L_y(\underline{U}^n) + L_z(\underline{U}^n) \quad , \tag{6}$$

where L_x, L_y, L_z are operators which involve taking differences in the x, y, and z directions, respectively, and the superscripts indicate the time level. An implicit difference approximation has the more general form

$$\underline{U}^{n+1} = \underline{U}^n + L_x(\underline{U}^n, \underline{U}^{n+1}) + L_y(\underline{U}^n, \underline{U}^{n+1}) + L_z(\underline{U}^n, \underline{U}^{n+1}) \tag{7}$$

As is indicated, the difference operations involve the time advanced (unknown) quantities as well as known quantities. In this case, the solution of the difference equations for $\underline{U}^{n+1}$ may involve solving a very large set of coupled algebraic equations. This is usually accomplished by either matrix techniques or iterative techniques. The

approach taken in MICE, is to use implicit difference operators, and to invoke an additional approximation known as time-step-splitting. In this approximation, the difference operators L_x, L_y, and L_z are applied sequentially instead of simultaneously. That is, we define intermediate values of $\underline{U}$, which we shall call $\underline{U}^{n+x}$, and $\underline{U}^{n+x+y}$, as follows:

$$\text{Step 1:} \quad \underline{U}^{n+x} = \underline{U}^{n} + L_x(\underline{U}^{n}, \underline{U}^{n+x}) \tag{8}$$

$$\text{Step 2:} \quad \underline{U}^{n+x+y} = \underline{U}^{n+x} + L_y(\underline{U}^{n+x}, U^{n+x+y}) \tag{9}$$

$$\text{Step 3:} \quad \underline{U}^{n+1} = \underline{U}^{n+x+y} + L_z(\underline{U}^{n+x+y}, U^{n+1}) \tag{10}$$

The error generated by this additional approximation of time-step-splitting is discussed in Appendix B.

Each of the above steps involve the application of one difference operator. The advantage, from a coding standpoint, of this approach, is that a single generalized "difference operator" subroutine can be written, which will perform any of the three steps above. The advantage from standpoint of core requirements, is that only the values corresponding to a single row or column of cells need be in main core at a given time. Thus, the number of computational cells which may be used for a given problem is limited not by main core size, but by the size of the ECS bank on the CDC 6600, or LCM on the 7600. One further advantage is that it becomes relatively easy to switch between doing 1-D, 2-D, and 3-D problems.

We shall now present the differential equations to which the one-dimensional difference operator must correspond. In these equations, the α_i are transport coefficients which are adjusted to improve the numerical stability of the code, Q is the artificial viscous pressure,

b and B are the parallel and perpendicular* magnetic field components, u and V are the parallel and perpendicular velocity components, $\rho^* = \rho + (B^2+b^2)/C_a^2$ is the so-called "Boris mass", and m = 0, 1. or 2, depending on whether the difference operator is being applied in planar, cylindrical, or spherical geometry.

The equations are:

$$\frac{\partial}{\partial t}(\rho) = -\frac{1}{x^m}\frac{\partial}{\partial x}\, x^m \left(\rho u - \alpha_1 \frac{\partial}{\partial x}\rho\right) \tag{11}$$

$$\frac{\partial}{\partial t}(b) = -u\frac{1}{x^m}\frac{\partial}{\partial x}\, x^m \left(b - \alpha_3 \frac{\partial}{\partial x} b\right) \tag{12}$$

$$\frac{\partial}{\partial t}(B) = -\frac{1}{x^m}\frac{\partial}{\partial x}\, x^m \left(Bu - \alpha_3 \frac{\partial}{\partial x} B\right) + b\frac{\partial}{\partial x} V \tag{13}$$

$$\frac{\partial}{\partial t}(\rho u) = -\frac{1}{x^m}\frac{\partial}{\partial x}\, x^m \left(\rho u^2 - \alpha_2\, \rho \frac{\partial}{\partial x}\, u\right)$$

$$- \frac{\partial}{\partial x}(P+Q) - \rho/\rho^* \frac{\partial}{\partial x}\left(\frac{B^2}{2}\right) - \rho\, G^* \tag{14}$$

where $G^* = \begin{cases} g, & \text{for vertical direction} \\ 0, & \text{otherwise} \end{cases}$,

$$\frac{\partial}{\partial t}(\rho V) = -\frac{1}{x^m}\frac{\partial}{\partial x}\, x^m \left(\rho V u - \alpha_2\, \rho \frac{\partial}{\partial x} V\right)$$

$$+ \rho/\rho^*\, b \frac{\partial}{\partial x} B \tag{15}$$

---

* We are considering only one perpendicular component of the velocity and B field. The generalization to two perpendicular components is straightforward.

$$\frac{\partial}{\partial t}(\rho I) = -\frac{1}{x^m}\frac{\partial}{\partial x}\, x^m \left(\rho I u - \alpha_4 \frac{\partial}{\partial x}\rho I\right)$$

$$- (P+Q)\frac{1}{x^m}\frac{\partial}{\partial x}\, x^m u \qquad (16)$$

or,

$$\frac{\partial}{\partial t}(E) = -\frac{1}{x^m}\frac{\partial}{\partial x}\, x^m \left(\{E+P+Q\}u - \alpha_4 \frac{\partial}{\partial x} E\right) - \rho\, G^* u$$

$$+ \rho/\rho^* \left(b\, V \frac{\partial}{\partial x} B - u \frac{\partial}{\partial x}\frac{B^2}{2}\right) \qquad (17)$$

where $E = \rho I + \frac{1}{2}\rho\left(u^2+V^2\right)$ (18)

The code may be run using difference forms of either equation (16) or equation (17) for the energy. The latter choice results in better energy conservation, but equation (16) gives more reliable temperatures in regions where magnetic forces dominate. The factor ρ/ρ^* which appears in front of the magnetic force terms has the effect of limiting the Alfven speed to the value C_a in regions where the mass density is very small. A limiting Alfven speed of 2×10^7 cm/sec has been found to be a satisfactory value.

The difference operator is constructed from these one dimensional differential equations. Multi-dimensional calculations are performed by suitably rotating the vector components in the routine which fetches the cell quantities from large core memory, so that the operator routine always "thinks" it is going in the x-direction.

L_x DIFFERENCE OPERATION

Another considerable simplification in the equations can be made by further splitting this set of equations into two sets, which

we will call "L_x phase 1" and "L_x phase 2." This splitting is done on the basis of the distinction between transverse Alfven waves and longitudinal or compressional Alfven waves. Phase 1 calculates the changes in the perpendicular components of B due to the propagation of transverse waves, while phase 2 calculates the changes in these components of B due to propagation of compressional waves. Phase 2 also calculates the changes in all other quantities.

The phase 1 equations are

$$\frac{\partial}{\partial t}(B) = b \frac{\partial}{\partial x} V \ , \tag{19}$$

and

$$\frac{\partial}{\partial t}(\rho V) = \rho/\rho^* \ b \frac{\partial}{\partial x} B \ . \tag{20}$$

For the case constant b and constant ρ, these equations are easily seen to be equivalent to the pair of 2nd order equations

$$\frac{\partial^2}{\partial t^2}(B) = \frac{b^2}{\rho^*} \frac{\partial^2}{\partial x^2}(B), \tag{21}$$

and

$$\frac{\partial^2}{\partial t^2}(V) = \frac{b^2}{\rho^*} \frac{\partial^2}{\partial x^2}(V) \ . \tag{22}$$

These are wave equations, representing waves traveling with velocity $\pm b/\sqrt{\rho^*}$. The amplitudes, V_0 and B_0, are related by the expression

$$B_0 = \sqrt{\rho^*} \ V_0 \ . \tag{23}$$

Each application of the difference operator results in the Phase 1 equations being solved implicitly for the (partially) time advanced values of B, after which the phase 2 equations are solved for the time advanced values of all of the cell quantities.

L_x PHASE 1 DIFFERENCING

The difference equations used in phase 1 for advancing the values of B are

$$\tilde{B}_j^{n+1} = B_j^n + \frac{\Delta t\, b_j^n}{\Delta x_j}\left[V_{j+\frac{1}{2}}^{n+\frac{1}{2}} - V_{j-\frac{1}{2}}^{n+\frac{1}{2}}\right], \tag{24}$$

and

$$V_{j+\frac{1}{2}}^{n+\frac{1}{2}} = V_{j+\frac{1}{2}}^n + \frac{\frac{1}{2}\Delta t\, b_{j+\frac{1}{2}}^n}{(\rho^*)_{j+\frac{1}{2}}^n \Delta x_{j+\frac{1}{2}}}\left[\tilde{B}_{j+1}^{n+1} - \tilde{B}_j^{n+1}\right], \tag{25}$$

where the integer subscripts refer to values at cell centers, half-integer subscripts refer to values at cell boundaries, and the superscripts refer to the time level. Cell boundary values are obtained by interpolation in the array of cell center values. These equations are solved for the quantities $\tilde{B}_j^{n+1}$, which are then used as initial values for L_x phase 2. These equations differ from the usual Lax-Wendroff two step form in that the right hand side of equation (25) contains the time-advanced values $\tilde{B}_j^{n+1}$. To obtain the solution, equation (25) is substituted into equation (24), giving the equation

$$\alpha_j \tilde{B}_{j+1}^{n+1} + \beta_j \tilde{B}_j^{n+1} + \gamma_j \tilde{B}_{j-1}^{n+1} = W_j, \tag{26}$$

where

$$\alpha_j = -\frac{(\Delta t)^2\, b_j^n\, b_{j+\frac{1}{2}}^n}{2\Delta x_j\, \Delta x_{j+\frac{1}{2}}\, (\rho^*)_{j+\frac{1}{2}}^n}, \tag{27}$$

$$\gamma_j = -\frac{(\Delta t)^2\, b_j^n\, b_{j-\frac{1}{2}}^n}{2\Delta x_j\, \Delta x_{j-\frac{1}{2}}\, (\rho^*)_{j-\frac{1}{2}}^n}, \tag{28}$$

$$\beta_j = 1 - \alpha_j - \gamma_j \quad , \tag{29}$$

and

$$W_j = B_j^n + \frac{\Delta t\, b_j^n}{\Delta x_j} \left[V_{j+\frac{1}{2}}^n - V_{j-\frac{1}{2}}^n \right] \tag{30}$$

The collection of equations (26) for all values of j, togother with the boundary conditions, constitutes a "tridiagonal" matrix, the solution to which is discussed in Appendix A. The boundary conditions are discussed in Appendix C.

L_x PHASE 2 DIFFERENCING

The phase 2 equations are equations (11) through (18), except that the second term on the right hand side of equation (13) is omitted, its effect having been accounted for in phase 1. The difference equations for phase 2 can be simplified by introducing symbols for the flux of mass, momentum, etc., as follows:

$$(\rho f)_{j+\frac{1}{2}}^{n+\frac{1}{2}} = (\rho u)_{j+\frac{1}{2}}^{n+\frac{1}{2}} - \frac{(\alpha_1)_{j+\frac{1}{2}}^n}{\Delta x_{j+\frac{1}{2}}} \left[\rho_{j+1}^{n+1} - \rho_j^{n+1} \right] \tag{31}$$

$$(\rho u f)_{j+\frac{1}{2}}^{n+\frac{1}{2}} = (\rho u)_{j+\frac{1}{2}}^{n+\frac{1}{2}} u_{j+\frac{1}{2}}^{n+\frac{1}{2}} - \frac{(\alpha_2)_{j+\frac{1}{2}}^n}{\Delta x_{j+\frac{1}{2}}} \left[\rho_{j+1}^{n+1} u_{j+1}^{n+1} - \rho_j^{n+1} u_j^{n+1} \right] \tag{32}$$

$$(\rho V f)_{j+\frac{1}{2}}^{n+\frac{1}{2}} = (\rho u)_{j+\frac{1}{2}}^{n+\frac{1}{2}} V_{j+\frac{1}{2}}^{n+\frac{1}{2}} - \frac{(\alpha_2)_{j+\frac{1}{2}}^n}{\Delta x_{j+\frac{1}{2}}} \left[\rho_{j+1}^{n+1} V_{j+1}^{n+1} - \rho_j^{n+1} V_j^{n+1} \right] \tag{33}$$

$$(bf)_{j+\frac{1}{2}}^{n+\frac{1}{2}} = b_{j+\frac{1}{2}}^n - \frac{\Delta t}{2} u_{j+\frac{1}{2}}^{n+\frac{1}{2}} \left(\frac{x_{j+1}^m b_{j+1}^n - x_j^m b_j^n}{x_{j+\frac{1}{2}}^m \Delta x_{j+\frac{1}{2}}} \right) \tag{34}$$

$$(bf')_{j+\frac{1}{2}}^{n+\frac{1}{2}} = - \frac{(\alpha_3)_{j+\frac{1}{2}}^n}{\Delta x_{j+\frac{1}{2}}} \left(b_{j+1}^{n+1} - b_j^{n+1} \right) \tag{34'}$$

$$(Bf)^{n+\frac{1}{2}}_{j+\frac{1}{2}} = B^{n+\frac{1}{2}}_{j+\frac{1}{2}}\ U^{n+\frac{1}{2}}_{j+\frac{1}{2}} - \frac{(\alpha_3)^n_{j+\frac{1}{2}}}{\Delta x_{j+\frac{1}{2}}}\left[B^{n+1}_{j+1} - B^{n+1}_{j}\right] \tag{35}$$

$$(Ef)^{n+\frac{1}{2}}_{j+\frac{1}{2}} = \left[E^{n+\frac{1}{2}}_{j+\frac{1}{2}} + (\gamma_{j+\frac{1}{2}} - 1)\ \rho^{n+\frac{1}{2}}_{j+\frac{1}{2}}\ I^{n+\frac{1}{2}}_{j+\frac{1}{2}} + Q_{j+\frac{1}{2}}\right] u^{n+\frac{1}{2}}_{j+\frac{1}{2}}$$

$$- \frac{(\alpha_4)^n_{j+\frac{1}{2}}}{\Delta x_{j+\frac{1}{2}}}\left[E^{n+1}_{j+1} - E^{n+1}_{j}\right] \tag{36}$$

with $E = \rho I + \frac{1}{2}\rho\,(u^2+v^2)$

$$(\rho If)^{n+\frac{1}{2}}_{j+\frac{1}{2}} = (\rho u)^{n+\frac{1}{2}}_{j+\frac{1}{2}}\ I^{n+\frac{1}{2}}_{j+\frac{1}{2}} - \frac{(\alpha_4)^n_{j+\frac{1}{2}}}{\Delta x_{j+\frac{1}{2}}}\left[\rho^{n+1}_{j+1}\ I^{n+1}_{j+1} - \rho^{n+1}_{j}\ I^{n+1}_{j}\right] \tag{37}$$

Equations (31) through (37) above define fluxes at the cell boundaries. Cell centered fluxes are defined in the MICE scheme as:

$$(\rho uf)_j = \rho^n_j \left(u^n_j\right)^2 , \tag{38}$$

$$(\rho Vf)_j = \rho^{n+1}_j\ u^{n+1}_j\ V^n_j , \tag{39}$$

$$(Bf)_j = B^n_j\ u^{n+1}_j , \tag{40}$$

and

$$(\rho If)_j = \rho^{n+1}_j\ I^n_j\ u^{n+1}_j . \tag{41}$$

The cell-boundary fluxes are time-centered, except for the additional transport terms involving the α's and differences of the time-advanced quantities. The α's have the form

$$\alpha_i = q_i \left\{ \left| \frac{\partial u}{\partial x} \right| + \left| \frac{\partial c}{\partial x} \right| \right\} (\Delta x)^2, \quad q_i \leq 1 , \tag{42}$$

Since these terms are of second order in Δx, we see that the cell-boundary fluxes are time-centered, to first order. The cell-centered fluxes, however, are mixtures of time n and time n+1 quantities. We therefore refrain from assigning a time level to the symbols for these fluxes.

We shall now write out the MICE difference equations, using difference operators defined as:

$$(\nabla\cdot)_j A \equiv \frac{1}{x_j^m \Delta x_j}\left[x^m_{j+\frac{1}{2}} A_{j+\frac{1}{2}} - x^m_{j-\frac{1}{2}} A_{j-\frac{1}{2}}\right] \tag{43}$$

$$(\nabla\cdot)_{j+\frac{1}{2}} A \equiv \frac{1}{x^m_{j+\frac{1}{2}} \Delta x_{j+\frac{1}{2}}}\left[x^m_{j+1} A_{j+1} - x^m_j A_j\right] \tag{44}$$

$$(D)_j A \equiv \frac{1}{\Delta x_j}\left[A_{j+\frac{1}{2}} - A_{j-\frac{1}{2}}\right] \tag{45}$$

$$(D)_{j+\frac{1}{2}} A \equiv \frac{1}{\Delta x_{j+\frac{1}{2}}}\left[A_{j+1} - A_j\right] \tag{46}$$

The difference equations are:

$$\rho_j^{n+1} = \rho_j^n - \Delta t\ (\nabla\cdot)_j\ (\rho f)^{n+\frac{1}{2}} \quad , \tag{47}$$

$$b_j^{n+1} = b_j^n - \Delta t\ u_j^{n+1}\ (\nabla\cdot)_j\ (bf)^{n+\frac{1}{2}} - \Delta t\ (\nabla\cdot)_j\ (bf')^{n+\frac{1}{2}} \tag{48}$$

$$B_j^{n+1} = B_j^n - \Delta t\ (\nabla\cdot)_j\ (Bf)^{n+\frac{1}{2}} \quad , \tag{49}$$

$$\rho_j^{n+1}\, v_j^{n+1} = \rho_j^n\, v_j^n - \Delta t(\nabla\cdot)_j\ (\rho u f)^{n+\frac{1}{2}} - \Delta t\ \rho_j^{n+1}\ G_j^*$$

$$- \Delta t\ (D)_j \left[(\gamma-1)\rho^{n+\frac{1}{2}}\ I^{n+\frac{1}{2}} + Q^n\right]$$

$$- \Delta t\left(\rho/\rho^*\right)_j^n\ (D)_j \left(\frac{B^2}{2}\right)^{n+\frac{1}{2}} \quad , \tag{50}$$

where $\left(\frac{B^2}{2}\right)^{n+\frac{1}{2}} \equiv B^{n+\frac{1}{2}}\, B^n - \frac{1}{2}\left(B^n\right)^2$,

$$\rho_j^{n+1}\, V_j^{n+1} = \rho_j^n\, V_j^n - \Delta t(\nabla\cdot)_j\ (\rho V f)^{n+\frac{1}{2}} + \Delta t(\rho/\rho^*)_j^n\, b_j^n\ (D)_j\ B^{n+\frac{1}{2}} \tag{51}$$

$$\rho_j^{n+1}\, I_j^{n+1} = \rho_j^n\, I_j^n - \Delta t(\nabla\cdot)_j\ (\rho I f)^{n+\frac{1}{2}}$$

$$-\Delta t\left\{(\gamma_j-1)\rho_j^{n+1}\ I_j^n + Q_j\right\}\ (\nabla\cdot)_j\ u^{n+\frac{1}{2}} \quad , \tag{52}$$

$$\rho_j^{n+1}\, E_j^{n+1} = \rho_j^n\, E_j^n - \Delta t(\nabla\cdot)_j\ (E f)^{n+\frac{1}{2}} - \Delta t\ \rho_j^{n+1}\ u_j^{n+1}\ G_j^*$$

$$+ \Delta t\left(\rho/\rho^*\right)_j^n \left[b_j^{n+1}\ V_j^{n+1}\ (D)_j\ B^{n+\frac{1}{2}} - u_j^{n+1}\ (D)_j\ \frac{B^2}{2}^{n+\frac{1}{2}}\right] \tag{53}$$

$$(\rho u)_{j+\frac{1}{2}}^{n+\frac{1}{2}} = (\rho u)_{j+\frac{1}{2}}^n - \frac{1}{2}\,\Delta t(\nabla\cdot)_{j+\frac{1}{2}}\ (\rho u^2)^n - \frac{1}{2}\,\Delta t\ \ \rho_{j+\frac{1}{2}}^n\ \ G_{j+\frac{1}{2}}^*$$

$$- \frac{1}{2}\,\Delta t(D)_{j+\frac{1}{2}} \left[(\gamma-1)\ \rho^n\ I^n + Q^n + n^2\ (\rho^{n+1} - \rho^n)\right]$$

$$- \frac{1}{2}\,\Delta t\left(\rho/\rho^*\right)_{j+\frac{1}{2}}^n\ \ (D)_{j+\frac{1}{2}} \left(\frac{B^2}{2}\right)^n \quad , \tag{54}$$

where $a^2 = \gamma(\gamma-1)\, I + B^2/\rho^*$ is the effective sound speed squared,

$$(\rho I)^{n+\frac{1}{2}}_{j+\frac{1}{2}} = (\rho I)^{n}_{j+\frac{1}{2}} - \frac{1}{2}\Delta t\,(\nabla\cdot)_{j+\frac{1}{2}}\,(\rho I f) - \frac{1}{2}\Delta t\left[(\gamma_{j+\frac{1}{2}} - 1)(\rho I)^{n}_{j+\frac{1}{2}} + Q_{j+\frac{1}{2}}\right](\nabla\cdot)_{j+\frac{1}{2}}\, u^{n+1}, \tag{55}$$

$$B^{n+\frac{1}{2}}_{j+\frac{1}{2}} = B^{n}_{j+\frac{1}{2}} - \frac{1}{2}\Delta t(\nabla\cdot)_{j+\frac{1}{2}}\,(Bf)\ , \tag{56}$$

and

$$(\rho V)^{n+\frac{1}{2}}_{j+\frac{1}{2}} = (\rho V)^{n}_{j+\frac{1}{2}} - \frac{1}{2}\Delta t\,(V\cdot)_{j+\frac{1}{2}}\,(\rho V f) + \frac{1}{2}\Delta t\left(\rho/\rho^*\right)^{n}_{j+\frac{1}{2}}\, b^{n}_{j+\frac{1}{2}}\,(D)_{j+\frac{1}{2}}\, B^{n+1} \tag{57}$$

The solution to the above difference equations is obtained algebraically substituting equations (54) and (31) into equation (47), obtaining a tri-diagonal set of equations for the ρ^{n+1}_j, which can then be solved. The quantities $\rho^{n+1}_{j+\frac{1}{2}}$ and $\rho^{n+\frac{1}{2}}_{j+\frac{1}{2}}$ are then calculated by interpolation in space and time. Having the values for ρ^{n+1}_j, equation (54) is then used to obtain $(\rho u)^{n+\frac{1}{2}}_{j+\frac{1}{2}}$, which, together with $\rho^{n+\frac{1}{2}}_{j+\frac{1}{2}}$, then gives the values for $u^{n+\frac{1}{2}}_{j+\frac{1}{2}}$.

Equations (32), (40), (41), (55), and (56) are combined algebraically with equation (50) to obtain a tri-diagonal set of equations which can be solved numerically for the quantities u^{n+1}_j. Equations (55) and (56) can then be used to obtain the quantities $(\rho I)^{n+\frac{1}{2}}_{j+\frac{1}{2}}$, and $B^{n+\frac{1}{2}}_{j+\frac{1}{2}}$. Equations (48) and (49) are then solved to find the new magnetic field components, after which, equation (57), and then equation (51), may be solved for the new perpendicular velocity components.

Then, finally, the energy equation is solved (equation (52) or equation (53), depending on which form is desired.)

When solving each of the above equations, the appropriate boundary conditions must be considered. Reflective boundaries and periodic boundaries are relatively straightforward, and are not discussed in this report. Transmittive boundaries are more troublesome, however, and the MICE treatment of such boundaries is discussed in Appendix C.

APPENDIX A

THE SOLUTION OF A TRI-DIAGONAL SYSTEM OF LINEAR EQUATIONS

A system of N linear equations is called tri-diagonal if it can be put in the form

$$A_j U_{j+1} + B_j U_j + C_j U_{j-1} = W_j \qquad 2 \leq j \leq N - 1 \tag{A1}$$

$$A_1 U_2 + B_1 U_1 = W_1 \tag{A2}$$

$$B_N U_N + C_N U_{N-1} = W_N \tag{A3}$$

where the U_j's are the unknown quantities, and A_j, B_j, C_j, and W_j are known. The equations may be ordinary scalar equations, or they may be matrix equations. Where equations of this form rise in HICE, equation (A1) represents the difference equations in the in erior of the mesh, while (A2) and (A3) are the boundary conditions.

The solution is obtained by introducing additional quantities X_j, Y_j, such that

$$U_{j+1} = X_j U_j + Y_j \tag{A4}$$

Substituting equation (A4) into equation (A1), we obtain

$$(A_j X_j + B_j) U_j + C_j U_{j-1} = W_j - A_j Y_j \tag{A5}$$

Raising the index j by one, and solving for U_{j+1}, we obtain

$$U_{j+1} = -\left(A_{j+1}X_{j+1} + B_{j+1}\right)^{-1} C_{j+1}U_j + \left(A_{j+1}X_{j+1} + B_{j+1}\right)^{-1}\left(W_{j+1} - A_{j+1}Y_{j+1}\right)$$

Comparing this expression with equation (A4), we make the identifications

$$X_j = -\left(A_{j+1}X_{j+1} + B_{j+1}\right)^{-1} C_{j+1} \quad , \text{ and} \tag{A6}$$

$$Y_j = \left(A_{j+1}X_{j+1} + B_{j+1}\right)^{-1}\left(W_{j+1} - A_{j+1}Y_{j+1}\right) .$$

Comparing equations (A3) and (A4), we see that

$$X_{N-1} = -\left(B_N\right)^{-1} C_N \quad , \text{ and}$$

$$Y_{N-1} = \left(B_N\right)^{-1} W_N .$$

Equations (A6) then give the X's and Y's for all smaller values of j. Equations (A4), with $j = 1$, is then combined with equation (A2), to give

$$U_1 = \left(A_1X_1 + B_1\right)^{-1}\left(W_1 - A_1Y_1\right) .$$

The U_j's for all higher values of j can then be found from (A4).

APPENDIX B

ANALYSIS OF THE ADDITIONAL ERROR GENERATED BY TIME-STEP-SPLITTING

For simplicity, let us consider the case of two-dimensional cartesian geometry. The differential equations we are attempting to solve can be put in the form

$$\frac{\partial}{\partial t} \underline{U} = \left(A \frac{\partial}{\partial x} + B \frac{\partial}{\partial y} \right) \underline{U} \quad , \tag{B1}$$

where the components of the vector $\underline{U}$ are the MHD dynamical variables ρ, I, V_x, V_y, B_x, B_y, and A and B are matrix functions of the components of $\underline{U}$. Then,

$$\frac{\partial^2}{\partial t^2} \underline{U} = \left(A \frac{\partial}{\partial x} + B \frac{\partial}{\partial y} \right) \frac{\partial}{\partial t} \underline{U} = \left(A \frac{\partial}{\partial x} + B \frac{\partial}{\partial y} \right)^2 \underline{U} \quad ,$$

and

$$\frac{\partial^m}{\partial t^m} \underline{U} = \left(A \frac{\partial}{\partial x} + B \frac{\partial}{\partial y} \right)^m \underline{U} \quad . \tag{B2}$$

A difference approximation to the differential equations has the form

$$\underline{U}^{n+1} = \Omega \left(\underline{U}^n, \underline{U}^{n+1} \right) \tag{B3}$$

where Ω is a difference operator, and the superscripts indicate the time level. The statement that Ω is accurate to order ℓ in Δt ,

means, mathematically, that if each term of the right hand side of equation (B3) is expanded in a Taylor series about time t^n, then the equation becomes

$$\underline{U}^{n+1} = \underline{U}^n + \Delta t \left(A\frac{\partial}{\partial x} + B\frac{\partial}{\partial y}\right)\underline{U}^n + \frac{\Delta t^2}{2}\left(A\frac{\partial}{\partial x} + B\frac{\partial}{\partial y}\right)^2 \underline{U}^n$$

$$+ \ldots + O\left(\Delta t^{\ell+1}\right) . \qquad \text{(B4)}$$

We say then, that $\Omega = I + \Delta t \left(A\frac{\partial}{\partial x} + B\frac{\partial}{\partial y}\right) + \frac{\Delta t^2}{2}\left(A\frac{\partial}{\partial x} + B\frac{\partial}{\partial y}\right)^2 + \ldots\ldots$

Now, let us suppose that we are given difference operators L_x and L_y, which correspond, respectively, to the differential equations

$$\frac{\partial}{\partial t}\underline{U} = A\frac{\partial}{\partial x}\underline{U} , \qquad \text{(B5)}$$

and

$$\frac{\partial}{\partial t}\underline{U} = B\frac{\partial}{\partial y}\underline{U} . \qquad \text{(B6)}$$

A non-time-split difference scheme would advance the values of U from time n to time $n+1$ by means of the operation

$$\underline{U}^{n+1} = \left(L_x + L_y\right)\left(\underline{U}^n, \underline{U}^{n+1}\right) .$$

In MICE, the operators L_x and L_y are applied sequentially, rather than simultaneously, however. That is,

$$\underline{U}^{n+x} = L_x\left(\underline{U}^n, \underline{U}^{n+x}\right)$$

$$\underline{U}^{n+1} = L_y\left(\underline{U}^{n+x}, U^{n+1}\right) = L_y\left(L_x\left(\underline{U}^n, \underline{U}^{n+x}\right), \underline{U}^{n+1}\right)$$

Now, let us suppose that L_x and L_y are individually accurate to second order. That is,

$$L_x = I + \Delta t\ A \frac{\partial}{\partial x} + \frac{\Delta t^2}{2} \left(A \frac{\partial}{\partial x}\right)^2 + 0\ (\Delta t^3)$$

$$L_y = I + \Delta t\ B \frac{\partial}{\partial y} + \frac{\Delta t^2}{2} \left(B \frac{\partial}{\partial y}\right)^2 + 0\ (\Delta t^3)$$

The "product" of these two operators, keeping terms up through order Δt^2 , is

$$\begin{aligned} L_y L_x &= I + \Delta t \left(A \frac{\partial}{\partial x} + B \frac{\partial}{\partial y}\right) \\ &\quad + \frac{\Delta t^2}{2} \left[\left(A \frac{\partial}{\partial x}\right)^2 + 2\ B \frac{\partial}{\partial y} A \frac{\partial}{\partial x} + \left(B \frac{\partial}{\partial y}\right)^2\right] \\ &= I + \Delta t \left(A \frac{\partial}{\partial x} + B \frac{\partial}{\partial y}\right) + \frac{\Delta t^2}{2} \left(A \frac{\partial}{\partial x} + B \frac{\partial}{\partial y}\right)^2 \\ &\quad + \frac{\Delta t^2}{2} \left(B \frac{\partial}{\partial y} A \frac{\partial}{\partial x} - A \frac{\partial}{\partial x} B \frac{\partial}{\partial y}\right) \end{aligned}$$

Thus, we see that there is an additional error introduced by the time-splitting. This error is of second order in Δt , and is given by

$$E = \frac{1}{2} \Delta t^2 \left(B \frac{\partial}{\partial y} A \frac{\partial}{\partial x} - A \frac{\partial}{\partial x} B \frac{\partial}{\partial y}\right) .$$

This is the lowest order error term caused by the time-splitting when the order of application of L_x and L_y is as indicated above. If the order of application is reversed, then $E \rightarrow -E$. This fact makes possible an easy check on the effects of this error term. To this end, two fireball rise calculations have been performed, differing from each other only in that the order of application of L_x and L_y was reversed. The results of these two calculations were essentially identical, indicating that the additional error generated by time-step-splitting can be ignored.

APPENDIX C

BOUNDARY CONDITIONS

The type of boundary which has always been difficult to handle properly is the out-flow, or "transmittive" boundary. Other types of boundaries can be treated in relatively straight-forward ways. Therefore, we will concentrate, in this appendix, on the MICE treatment of the transmittive boundary.

At points which are outside the space mesh, we are either not interested in the values of the dynamical variables, or we decide not to attempt to compute them, on the basis of lack of computing capability. In any case, since the size of computer memories is finite, there must always be an "outer boundary" beyond which lie space points for which we have no detailed information. Therefore, some assumption must be made at the outer boundary, in order to be able to compute in the cells adjacent to the boundary.

In the MICE code, the following assumptions have been imposed at the outer boundaries:

(i) There can be no "inflow" of mass.

(ii) The time rate of change of the amplitude of incoming waves is zero.

These conditions seem to allow signals to propagate out of the mesh without causing excessive disturbances within the mesh.

In phase 1, where transverse Alfven waves are treated, only condition (ii) above is applicable. Let us consider a row of cells, numbered from 1 to JMAX, with J increasing from left to right. In cell no. JMAX, we want the time rate of change of the amplitude of

the left-going wave to be zero. Now, the phase 1 differential equations can be written

$$\frac{\partial}{\partial t}\left(B_\perp\right) = B_x \frac{\partial}{\partial x}\left(V_\perp\right) \tag{C1}$$

and

$$\frac{\partial}{\partial t}\left(V_\perp\right) = \frac{B_x}{\rho^*} \frac{\partial}{\partial x}\left(B_\perp\right) , \tag{C2}$$

Where $\rho^* = \rho + B^2/C_a^2$ and $V_\perp$, $B_\perp$ are the components of V and B perpendicular to the x-direction. To simplify the boundary treatment, we consider B_x and $\rho^*$to be constant. Equations (C1) and (C2) above are then equivalent to the pair of equations

$$\frac{\partial}{\partial t}\left(B_\perp + \sqrt{\rho^*}\, V_\perp\right) = \frac{B_x}{\sqrt{\rho^*}} \frac{\partial}{\partial x}\left(B_\perp + \sqrt{\rho^*} V_\perp\right) , \tag{C3}$$

and

$$\frac{\partial}{\partial t}\left(B_\perp - \sqrt{\rho^*} V_\perp\right) = -\frac{B_x}{\sqrt{\rho^*}} \frac{\partial}{\partial x}\left(B_\perp - \sqrt{\rho^*} V_\perp\right) . \tag{C4}$$

Equation (C4) states that constant values of $B_\perp - \sqrt{\rho}\, V_\perp$ travel along paths with $X - \frac{B_x}{\sqrt{\rho^*}} t =$ constant, while (C5) states that the quantity $B_\perp + \sqrt{\rho^*}\, V_\perp$ is constant along $X + \frac{B_x}{\sqrt{\rho^*}} t =$ constant. At the right hand boundary, for the case $B_x > 0$, $B_\perp + \rho^* V_\perp$ is the amplitude of the incoming wave. Condition (ii) above then becomes

$$\frac{\partial}{\partial t}\left(B_\perp + \sqrt{\rho^*} V_\perp\right) = 0 . \tag{C5}$$

Another equation is needed in order to establish the rates of change of $B_\perp$ and $V_\perp$ individually, and we have arbitrarily chosen to use the equation

$$\frac{\partial}{\partial t}\left(B_\perp\right) + \frac{|B_x|}{\sqrt{\rho^*}} \frac{\partial}{\partial x}\left(B_\perp\right) = 0 \quad . \tag{C6}$$

This equation is implemented in the following way: One goes back into the mesh a distance $\frac{B_x}{\sqrt{\rho^*}} \Delta t$, picks up the value of $B_\perp$ from from that point, and uses that value for the new $B_\perp$ at the right hand boundary. Equation (C5) then determines the new value of $V_\perp$.

This treatment produces the wrong value for the amplitude of the outgoing wave, but gets the desired value for the amplitude of the incoming wave. In principle, equation (C4) could be employed to obtain the correct value for the amplitude of the outgoing wave, but experience shows that attempts to assign values to both incoming and outgoing waves can produce values at the boundary which are obviously non-physical. The method we have chosen is less likely to cause numerical instabilities at the boundary, even though it is not strictly mathematically correct.

The above is a description of the right-hand boundary treatment for $B_x > 0$. Other cases are treated in an analagous way.

The phase 2 equations,

$$\frac{\partial}{\partial t}(\rho) + \frac{\partial}{\partial x}(\rho V_x) = 0$$

$$\frac{\partial}{\partial t}(\rho V_x) + \frac{\partial}{\partial x}(\rho V_x^2 + P^*) = 0$$

$$\frac{\partial}{\partial t}\ (I) \ + \ V_x \frac{\partial}{\partial x}\ (I) \ + \ \frac{p}{\rho}\ \frac{\partial}{\partial x}\ (V_x) \ = \ 0$$

with $$p' \ = \ p \ + \ \rho/\rho^* \ \frac{B_I^2}{2} \quad , \quad \text{and}$$

$$p \ = \ (\gamma - 1)\ \rho I \ ,$$

can be put in the form

$$\frac{\partial}{\partial t}\ \left(I\ \rho^{-(\gamma-1)}\right) \ + \ V_x \frac{\partial}{\partial x}\ \left(I\ \rho^{-(\gamma-1)}\right) \ = \ 0 \qquad (C7)$$

$$\frac{\partial}{\partial t}\ (\sigma + V_x) \ + \ (V_x + C)\ \frac{\partial}{\partial x}\ (\sigma + V_x) \ = \ 0 \qquad (C8)$$

$$\frac{\partial}{\partial t}\ (\sigma - V_x) \ + \ (V_x - C)\ \frac{\partial}{\partial x}\ (\sigma - V_x) \ = \ 0 \qquad (C9)$$

where $$C \ = \ \left(\gamma(\gamma-1)\ I \ + \ \frac{B_I^2}{\rho^*}\right)^{-1/2}$$

and $$\sigma \ = \ \int \frac{dp'}{\rho c} \ .$$

These equations have the interpretation that the three quantities $I\ \rho^{-(\gamma-1)}$, $\sigma + V_x$, and $\sigma - V_x$, are each constant along characteristic curves whose slopes are

$$\frac{dx}{dt} \ = \ V_x \ , \quad \frac{dx}{dt} \ = \ V_x + C \ , \quad \text{and} \quad \frac{dx}{dt} \ = \ V_x - C \ ,$$

respectively. Again confining our attention to the right hand boundary, we must have $\frac{\partial}{\partial t}\ (\sigma - V_x) \ = \ 0$, to satisfy condition (11). This causes equation (C9) to be satisfied, since we assume that the amplitude

of the incoming wave is zero. The other equations which we use at the right hand boundary are

$$\left(\frac{\partial}{\partial t} + V_x \frac{\partial}{\partial x}\right) \rho = 0 , \tag{C10}$$

and

$$\left(\frac{\partial}{\partial t} + V_x \frac{\partial}{\partial x}\right) I = 0 . \tag{C11}$$

If ρ and I satisfy these equations, then equation (C7) is satisfied. Equation (C8), which describes outgoing waves, is not satisfied, but this is apparently not as important as meeting the condition of no incoming waves.

Equations (C10) and (C11) are satisfied by moving the distance $V_x \Delta t$ in from the boundary, picking up the values of ρ and I from that point, and using these as the new boundary values. Then, the new value of V_x at the boundary is chosen to satisfy $\Delta(\sigma - V_x) = 0$, with the restriction that V_x in the boundary cell cannot exceed V_x in the first cell inside the boundary.

The above described method of treating transmittive boundaries gives satisfactory results, both for strong shocks and weak shocks passing through the boundary.

REFERENCES

1. D. H. Sowle, et. al., "Effects of High Altitude Nuclear Explosions", DASA Reports, DASA 2453 and DASA 2593.

2. F. H. Harlow and B. D. Meixner, "Rise through the Atmosphere of a Hot Bubble", Los Alamos Report LAMS-2770.

3. D. S. Sappenfield, "A Two-Dimensional Hydrodynamic Model for an Explosion in a Non-Uniform Atmosphere", Los Alamos Report LA4189MS.

4. C. Longmire, et. al., "An Accurate Early Time Solution for a Rising Fireball Model," MRC report MRC-R-20, also published as DNA2967T.

5. F. H. Harlow and A. A. Amsden, "A Numerical Fluid Dynamics Calculation Method for All Flow Speeds", J. Comp. Physics, accepted for publication.